

Measurements of detector nonlinearity at 193 nm

Holger Laabs, Darryl A. Keenan, Shao Yang, and Marla L. Dowell

We have developed a measurement system based on a correlation method to characterize the nonlinearity of a detector's response over a large range of laser pulse energy. The system consists of an excimer-laser source, beam-shaping optics, a beam splitter, a monitor detector, a set of optical filters, and the detector under test. Detector nonlinearities as large as 10% or greater over an entire measurement range at an excimer-laser wavelength of 193 nm are observed. The measurement range of the current system is approximately 300 nJ to 50 mJ of laser pulse energy at the detector under test. The typical expanded measurement uncertainty of nonlinearity is 0.6% ($k = 2$).

OCIS codes: 040.7190, 120.3930, 120.4800.

1. Introduction

To meet the semiconductor industry's demands for accurate excimer-laser measurements, we have developed a system for measuring the nonlinear response of radiation detectors for UV light from an excimer-laser source. This system, which complements other National Institute of Standards and Technology (NIST) excimer-laser power and energy calibration services,¹⁻⁵ provides a quantitative measurement of a detector's response over a large energy range. Most detectors are typically used over an energy range that is larger than the range covered by the calibration. The measurement error is introduced if the detector response is not linear and the nonlinearity is not quantified. Range discontinuity, e.g., due to a change in detector amplification, can introduce additional measurement error. Quantitative determination of these performances of a detector can improve measurement precision and the estimation of measurement uncertainty. Possible sources of detector nonlinearity include the dependence of detector response on input signal, the range discontinuity of the detector system or read-out electronics, and background noise.

The energy E of a laser pulse measured by the detector of an energy meter can be expressed as

$$E = f(V), \quad (1)$$

where V is the voltage signal from the detector in response to the incident laser pulse energy E and $f(V)$ is the inverse of the detector response function, $V = g(E)$, and determines the detector nonlinearity. The term $f(V)$ is related to the calibration factor $F = V_c/E_c$ by $f(V_c) = V_c/F$. Subscript c indicates values of V or E in fixed calibration conditions. The calibration factor F is determined by comparing the detector response V_c with that of a NIST primary or transfer standard, henceforth referred to as a standard, at E_c . In many practical cases the nonlinear function $f(V)$ of a detector can be represented by a polynomial,

$$f(V) = a_0 + a_1V + a_2V^2 + \dots + a_nV^n. \quad (2)$$

When all the coefficients of a except a_1 , are zero, the detector is linear; a_0 is the background reading.

There are a variety of methods for characterizing the nonlinearity of a detector's response. In the most straightforward way the comparison method calibrates the detector response against a standard at several pulse energies. The data are fit to Eq. (1) by using a least-squares method to determine the function $f(V)$ or, in the case of a polynomial, the coefficients a_i in Eq. (2). Nonzero coefficients of higher order are a measure of the detector's nonlinearity. However, the dynamic range of the comparison method is limited to the usable energy range of the standard detector. In addition this method is time consuming because a full calibration is performed for each data point. Other more practical methods where standard detectors are not required are more commonly used in characterizing the response nonlinearities of detectors.⁶⁻⁹

The authors are with the Optoelectronics Division, National Institute of Standards and Technology, 325 Broadway, Boulder, Colorado 80305-3328 (e-mail for S. Yang, syang@boulder.nist.gov).

Received 25 August 2004; revised manuscript received 30 September 2004; accepted 3 October 2004.

In the superposition method a set of triplet measurements is taken that results in a set of data (V_1, V_2, V_3) , where V_i is the detector response owing to measurement of incident pulse energy E_i :

$$E_3 = E_1 + E_2. \quad (3)$$

If $V_3 = V_1 + V_2$, the detector is linear within an energy range spanned by the three pulse energies. The triplet measurement is repeated many times at different energy levels to yield information concerning the detector's nonlinearity across the entire measurement range. The superposition method has been used to characterize optical-fiber power meters in the near-IR wavelength range.⁶ However, a stable source of laser power or energy is essential to the superposition method. Therefore it is impractical to apply this method to excimer-laser detectors because of large pulse-to-pulse energy fluctuations in most common excimer lasers.

With the attenuation method^{7,8} the pulse energy is varied by an attenuator, such as an adjustable pinhole aperture, a moving knife-edge, a chopper, an absorbing material, or an optical filter. The deviation of the apparent attenuation, the ratio of the detector outputs corresponding to the attenuated and not-attenuated beam inputs, from the true attenuation of the attenuator is a measure of detector nonlinearity. So this method requires the attenuation of the attenuator to be precisely determined, stable, and durable. To determine their attenuation, geometrical attenuators require prior knowledge of the laser beam profile.⁷ The unstable pulse-to-pulse output and spatial beam profile of the excimer laser and the damaging effect of high-power UV light on optical materials make it difficult to implement the attenuation method with desired uncertainty for detector linearity measurement in the UV region with an excimer laser as the source.

We have developed a new method dubbed the correlation method and a measurement system based on this method, where the response of a device under test (DUT) is compared with a monitor detector whose response is linear within a limited range. The correlation of the two detectors' signals provides a quantitative measurement of the nonlinearity of the DUT. One challenge of this method is minimizing the uncertainty in the characterization of the monitor detector's linearity such that its contribution to the overall uncertainty is minimal.

2. Determination of Detector Nonlinearity by the Correlation Method

In laser calibration, instead of Eq. (1), energy E is alternatively expressed as⁹

$$E = \frac{V}{F \text{CF}(V)}, \quad (4)$$

where $\text{CF}(V)$ is called the correction factor, which

accounts for the effect of detector nonlinearity and is therefore an appropriate representation of detector nonlinearity. Unlike other methods the correlation method measures $\text{CF}(V)$ in Eq. (4) directly to characterize detector nonlinearity. Using $\text{CF}(V)$ to express detector nonlinearity implies that the nonlinearity is determined with reference to the calibration point V_c of the detector, where the calibration is performed. In other words, calibration factor F has been determined, and the correction factor $\text{CF}(V_c)$ is one by definition. However, the response nonlinearity is a relative property of the detector; that is, a multiplication factor applied to $\text{CF}(V)$ does not change the nonlinearity behavior that it represents, and therefore the reference point can be any point that is convenient. So when $\text{CF}(V)$ is used purely for the purpose of expressing detector nonlinearity instead of correcting the calibration factor, the calibration point V_c may be replaced by a reference point V_r . When it is necessary to indicate which specific reference point V_r is used, $\text{CF}(V)$ may be expressed as $\text{CF}(V; V_r)$. The detector response is linear if $\text{CF}(V) \equiv 1$.

The correlation method requires a monitor detector with linear response, which receives part of the laser beam from a beam splitter. The energy E of the beam incident on the test detector is related to the detector output V through Eq. (4) and is linearly proportional to the corresponding output V_m of the monitor detector, which is linear:

$$E = \alpha V_m. \quad (5)$$

Factor α is a constant determined by the response of the monitor detector, the beam-splitter ratio, and the attenuation of the optical components in both beam paths. Eliminating E in Eqs. (4) and (5) gives

$$\text{CF}(V) = \frac{V}{F} \frac{1}{\alpha V_m}. \quad (6)$$

Equation (6) holds for all V and V_m including the reference point as long as α is constant. The correction factor is one at the reference point, where the outputs of the test and the monitor detectors are V_r and V_{mr} , respectively:

$$\text{CF}(V_r) = \frac{V_r}{F} \frac{1}{\alpha V_{mr}} = 1. \quad (7)$$

Equations (6) and (7) lead to

$$\text{CF}(V) = \frac{V}{V_m} \frac{V_{mr}}{V_r}. \quad (8)$$

Dictating how the correction factor is measured, Eq. (8) is the basic expression for the correlation method. The measured $\text{CF}(V)$ can easily be expressed with a new reference point, say the calibration point V_c when the calibration has been performed:

$$CF(V; V_c) = \frac{V}{V_m} \frac{V_{mr}}{V_r} \frac{V_r}{V_{mr}} \frac{V_{mr}}{V_c} = \frac{CF(V; V_r)}{CF(V_c; V_r)}. \quad (9)$$

The correlation method is valid with the assumption that the monitor detector is linear. However, most, if not all, detectors are to some degree not linear. The chosen monitor detector is measured to be linear with some uncertainty. Usually the wider the range of a detector to be used, the larger its nonlinearity or the uncertainty with which it is tested. To minimize the effect of its nonlinearity, the monitor detector should be used within a limited range, e.g., no more than one order of magnitude. Since the range of the detector to be tested is usually much larger than this limited range of the monitor, the nonlinearity over the entire range of the test detector is measured in several measurement spans, each corresponding to the same limited monitor detector range. For one measurement span to be changed to the next, the optical filters in the DUT beam path have to be varied while the monitor path is kept unchanged. So, the factor α in Eq. (5) can be kept constant only within one span and is different from one span to another. Furthermore there is no single reference point common to all the spans. Therefore Eq. (8) cannot be used for all the spans. To express the nonlinearity $CF(V)$ for all the measurement spans with a single reference point, we use partially overlapped spans. When one span of measurement is completed where the reference point common to all the measurement spans is to be located, we adjust the attenuators so that the next span has a small region to overlap part of the previous span. In the region common to both spans a point V_r can be picked to serve as a transitional reference point for the new span. Instead of Eq. (7) we now have in the new span

$$CF(V_{r'}) = \frac{V_{r'}}{F} \frac{1}{\alpha V_{mr'}}. \quad (10)$$

$CF(V_{r'})$ was determined in the previous span of measurement and does not in general equal one. Replacing Eq. (7) with Eq. (10) in the derivation of Eq. (8), we now obtain Eq. (11) for the spans of measurements that do not include the common reference point V_r :

$$\begin{aligned} CF(V; V_r) &= \frac{V}{V_m} \frac{V_{mr'}}{V_{r'}} CF(V_{r'}; V_r) \\ &= CF(V; V_{r'}) CF(V_{r'}; V_r). \end{aligned} \quad (11)$$

With Eqs. (8) and (11) the nonlinearity measurement can be extended to the entire range of the detector with a single common reference point V_r .

The correlation method determines the correction factor $CF(V)$ at discrete points. Correction factors at intervening points can be obtained by interpolation or curve fitting. Together with the absolute calibration

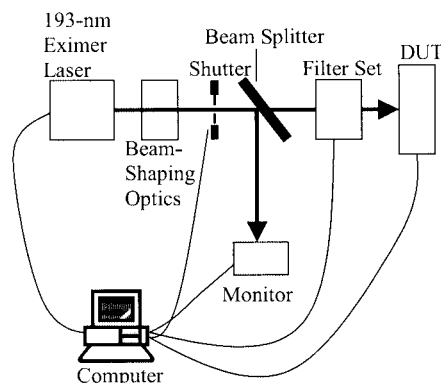


Fig. 1. Nonlinearity measurement system. The laser power change, shutter operation, filter set change, and data collection from DUT and monitor detector are controlled by the computer. The measurement process is fully automated.

at one or a few points the detector is now calibrated over the entire range covered by the nonlinearity measurement.

3. Calibration System and Procedure

Figure 1 illustrates our calibration system consisting of an ArF excimer laser, beam homogenization optics, the monitor detector, the standard detector, a beam splitter, and a set of attenuators. The laser has a pulse width of ~ 10 ns and maximum pulse energy of 100 mJ. Effects due to spatial fluctuations in the laser beam intensity are removed by incorporating beam homogenization optics into the optical path of the calibration system.^{5,10,11} However, beam homogenization is not essential in the correlation method if the beam size is smaller than the DUT sensor, and the monitor sensor detector uniformity is not a concern. The dimensions of the square-shaped laser beam profile (13×13 mm) are selected such that a variety of DUT sizes can be accommodated. In addition the beam size can be adjusted so that the active region of the DUT is either overfilled or underfilled. The maximum laser pulse energy incident on the test detector is ~ 50 mJ and the minimum pulse energy 300 nJ, determined by the maximum attenuation. The monitor detector is used in the range of 3–30 mV of its output.

Because of the instability of the pulse energy of the UV excimer laser, the measurement data exhibit large noise. To reduce the effect of the noise, hundreds of data points are acquired. Also, because of the noise, we do not use any particular data point as the reference of the measured $CF(V)$. Instead we use a virtual point, which is the average of the measurement results, as the reference. This approach is based on the understanding that nonlinearity is a relative feature of the detector as we mentioned above.

Although it is not necessary, measurements of the correlation method usually start with the highest or lowest meter range to be characterized. When the first measurement span is completed, filters are adjusted for the next span, which has part of its range

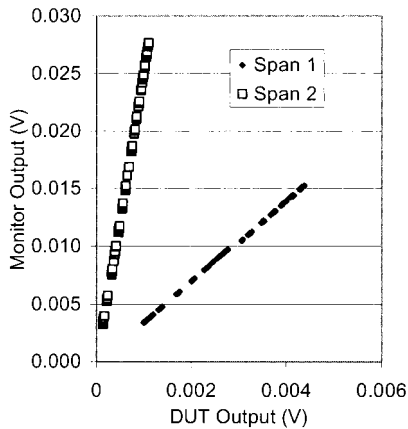


Fig. 2. Example of measured data pairs of the voltage outputs from the monitor detector and DUT in two measurement spans. The output of the monitor detector for the two spans is within the same voltage range, while the output of the DUT for the two spans is extended through approximately 1.5 meter ranges with a small common region. The DUT meter range changed at a DUT output of 3 mV during data collection for Span 1.

overlap with part of the previous span. The common region of the two adjacent spans serves to extend the $CF(V)$ measure from one span to the next with reference to the same point. The measurement span range does not usually coincide with the DUT meter ranges. So in the middle of some of the spans it is necessary to switch the meter range, and a gap due to the range discontinuity of the meter in the $CF(V)$ plot may appear. Figure 2 illustrates the measured DUT and monitor output data pairs for two spans. The two spans cover more or less the same output range on the vertical scale that is the monitor output. The DUT output on the horizontal axis extends for ~ 1.5 orders of magnitude with overlaps between neighboring spans. Figure 3 is the measured $CF(V)$ of the two spans, each with reference to its own average. The range discontinuity can be seen on Span 1.

The measured $CF(V)$ for all the spans on the same DUT do not have the same reference point after the

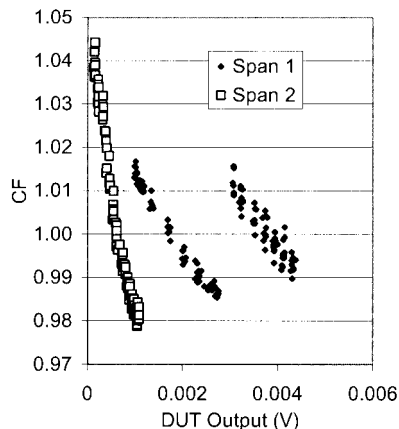


Fig. 3. Calculated nonlinearity of $CF(V)$ of the two spans. Each span has the average $CF(V)$ as its reference point. The range discontinuity at 3-mV DUT output is distinctly seen.

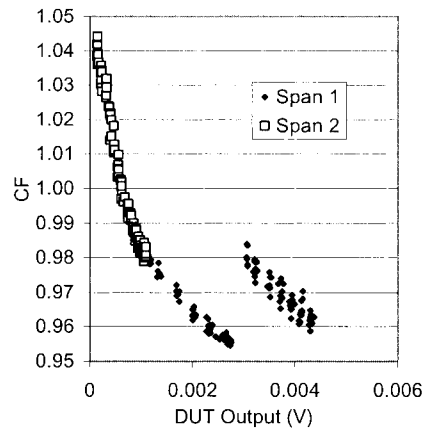


Fig. 4. Nonlinearity $CF(V)$ of the two spans is matched by moving the data of Span 1 to minimize the difference in the common region. The basic feature of the nonlinearity does not change in the match. The result is the same if we move the data of Span 2 to perform the match, but the vertical scale is different.

data acquisition as shown in Fig. 3. In principle we can use Eq. (11) to make all the $CF(V)$ referenced to the same point V_r via points V_r' in the common regions of neighboring spans. However, because of the noise, one single point V_r' in the common region causes large uncertainty in the use of Eq. (11). A sizable number of data points in the common region make it possible to match the common regions of the two adjacent spans statistically. Apply a multiplication factor to the span that does not contain the desired reference point V_r , until the statistical difference in the data in the common region of the two spans is minimized. Figure 4 is the result of this statistical match of the two curves in Figure 3. This process is repeated until the farthest measurement span is reached.

The next step in data processing is curve fitting. With a gap between neighboring ranges of the detector meter, curve fitting should be applied to each meter range separately. Although other functions may be used for the curve to be fitted, we found that a polynomial is almost always sufficient for the purpose. In the data-processing program we fit the $CF(V)$ data with several different orders of polynomials at the same time. A statistical F -test number is listed along with plots of the fitted curve on top of the $CF(V)$ data points. The F -number together with visual observation determines which order of polynomial is accepted. Figure 5 shows the curve-fitting results of our example.

If the absolute calibration of the detector is performed, whether before or after the nonlinearity measurement, we can extend the calibration to the entire meter range with the nonlinearity information by simply finding $CF(V_c)$ from the fitted curve and using it in Eq. (9). Absolute calibration has a lower uncertainty than nonlinearity measurements, especially when the nonlinearity measurement extends to several spans. However, the latter is faster and gives complete information in the entire measured range.

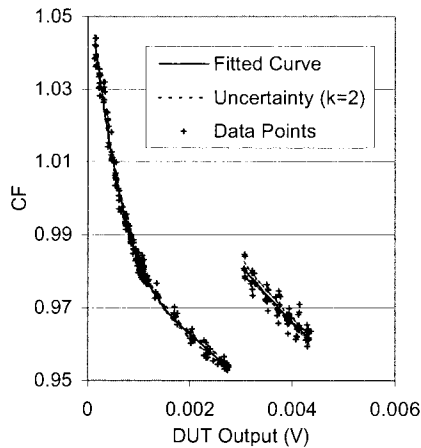


Fig. 5. Curve-fitting results (solid curve) of the matched CF(V) data in Fig. 4. Curve fitting is done separately in the two ranges. The range discontinuity is $\sim 3\%$. The dashed curves along the fitted curve are the limits of uncertainty ($k = 2$).

When a detector is to be characterized in a wide range, the overall uncertainty may not meet the required specification if absolute calibration is performed at only one point V_c and calibration is extended to points far from it with nonlinearity measurement. It may be necessary to run absolute calibration at points in more than one measurement range of the detector to meet the uncertainty specification.

The optical detectors might have a background reading even when they receive no laser light signal. This background signal could be caused by ambient light, acoustic or rf interference, or an offset in the electronic circuitry. A special problem in this respect with the laser pulse meters is that, in measurements with input signal triggering, the background is hidden; that is, it does not show up because the noise is not high enough to trigger the meter. We used pulses with the same repetition rate as the laser signal to trigger the pulse meter externally to characterize the statistical distribution of the background reading, which is expected to be or close to Gaussian. Because the background is close to zero, noise associated with it may spread to negative values. Evaluation of its mean value may not be as simple as averaging a number of readings because many meters do not display negative readings. For meters without negative readings the Gaussian is truncated at zero and the full Gaussian should be reinstated. The mean value of the background that may affect the measurement signal is the peak of the Gaussian, truncated or not, instead of the average of the readings. The background uncertainty is the standard deviation of the full Gaussian. Background characterization may have to be carried out at each meter range because it might be different for each range. Figure 6 shows an example of the background output of a pulse laser energy meter measured with external triggering.

The effect of the background on the signal output is a complex combination of the origin(s) of the background, its characteristics (frequency spectrum and

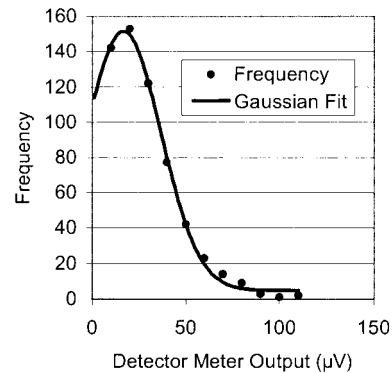


Fig. 6. Monitor detector background reading test result. The frequency of the pulse energy meter output has a truncated Gaussian distribution with the peak at $\sim 17 \mu\text{V}$ and a standard deviation of $29 \mu\text{V}$. The frequency of a zero reading of 601, which accounts for the frequencies of true zero and all the negative readings, is not shown.

phase), and signal processing. In many cases its effect may not be corrected with simple subtraction of the measured background from the signal. The effect of background signal is better treated as part of detector nonlinearity. Since the effect of background reading depends on the environment of the meter application, the characterization of the background or the detector nonlinearity should be carried out in similar conditions.

4. Uncertainty Assessment

The overall uncertainty of CF(V) is composed of the uncertainties of individual components in Eqs. (8) and (11). The data pair of V and V_m is partially correlated because it varies simultaneously with laser output fluctuations. So uncertainties in the ratios of these data pairs, instead of uncertainties in the individual data, are the real contributors to the total uncertainty. For the same reason the uncertainties in the ratios that we have observed so far are between 0.5% and 1.5% depending on the DUT and the ranges used; the uncertainties are much smaller than those of the individual datum even though the pulse-to-pulse spread of the laser output is more than 10%. This is the primary source of the measurement uncertainty of the correlation method. The secondary sources are statistical matching of the common regions of adjacent spans and curve-fitting uncertainties. Another source of uncertainty is the assumption that the monitor detector is linear.

The uncertainty in the statistical matching of the common regions of adjacent spans can be estimated by $[(\Delta_1)^2/n_1 + (\Delta_2)^2/n_2]^{1/2}$, where Δ_1 and Δ_2 are the standard deviations of V/V_m in the matching regions of the two adjacent spans and n_1 and n_2 are the number of data points in the two regions. With the typical number of n_1 and n_2 being 25 and Δ_1 and Δ_2 1% the matching uncertainty is 0.28%. Each time when two spans are matched this uncertainty should be estimated and added to the total uncertainty of the next extended span.

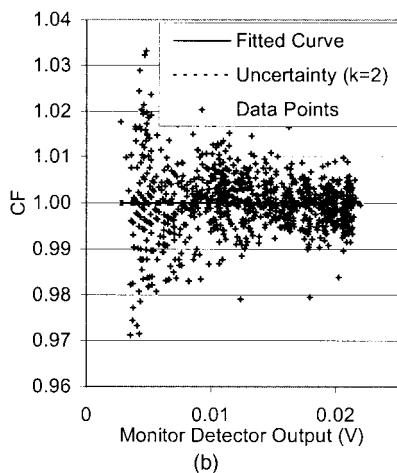
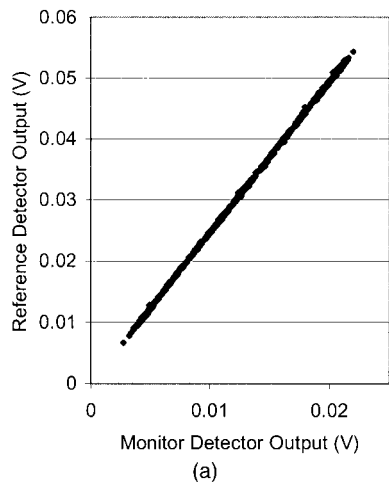


Fig. 7. Linear correlation between the monitor detector and one of the reference detectors: Top, measured data; bottom, calculated $CV(V)$ and the fitted curve. The fitted curve coincides with the horizontal line of $CF = 1$. With 930 data points the fitting uncertainty is very low, although the data are quite noisy.

The uncertainty in the curve-fitting result is calculated by using the normal statistical procedure.¹² In Fig. 5 the two dotted curves above and below the solid fitted curve show the expanded uncertainty ($k = 2$) of the fitted curve, where the maximum uncertainty ($k = 1$) is $\sim 0.1\%$. The data-processing program includes the calculation of the uncertainty of the curve-fitting result.

To verify its linearity, the monitor detector was tested against several other detectors, i.e., its response was measured against various other detectors including a primary standard calorimeter in the same measurement system of this correlation method. If the responses of detectors of various combinations were highly linearly correlated, i.e., the best fit of $CF(V)$ was a horizontal straight line at 1, either all the detectors had identical nonlinearity or they were all linear in response within the measurement uncertainties. The more detector combinations tested, the smaller the chance of having detectors with the same nonlinearity. Figure 7 is an example of the test of the linearity of the monitor detector. Al-

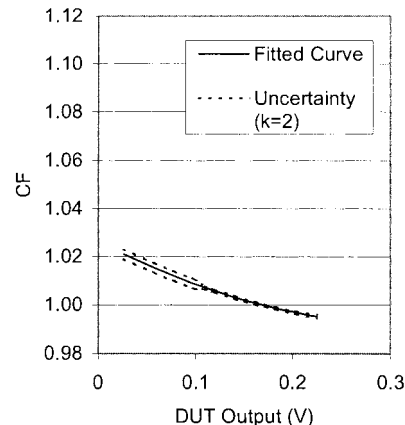


Fig. 8. Measured detector nonlinearity of Detector 1. The measurement covers one meter range. The nonlinearity in this range is $\sim 2.5\%$. The maximum expanded uncertainty ($k = 2$) is $\sim 0.2\%$. The sharp change in the middle of the uncertainty curve is due to the measurement span match.

though the data are quite noisy the uncertainty in the linear fitting is very low, $\sim 0.05\%$, because of the large number, 930, of data points.

The linear correlation uncertainty is the combination or statistical sum of the uncertainties of data from the two test detectors. If one of the detectors is perfectly free of noise and linear, this combined uncertainty is contributed purely from the other test detector. Therefore the best estimate of the test uncertainty of the monitor detector nonlinearity is the smallest number of combined uncertainties where the monitor detector is one of the test components.

If $CF(V)$ is used purely for nonlinearity characterization, the total uncertainty is the combination of the uncertainty of the fitted curve, the matching uncertainty if any, and the uncertainty of the monitor detector nonlinearity. However, if it is used as a correction factor of the calibration factor F in Eq. (4), the uncertainty in $CF(V_c)$ must be added onto the uncertainty estimated for the nonlinearity feature. The estimation of the uncertainty in $CF(V_c)$ is the same as for any other point but without the uncertainty of statistical matching. The typical total expanded uncertainty ($k = 2$) with one scan matching is $\sim 0.6\%$ for nonlinearity $CF(V)$ and 0.63% for calibration factor correction.

There are two types of uncertainties when the contributions are assessed from different sources.¹³ Type A uncertainties are those that can be directly assessed by statistical methods from the measurement data. Type B uncertainties are those estimated based on scientific judgment when all the relevant information available is used. Uncertainties in the correlation method are all Type A.

5. Measurement Results

Figures 8–11 are the final fitted curves of the measurement results of four UV pulse energy meters with pyroelectric detectors of different manufacturers. Figures 8–11 have the same vertical scale to

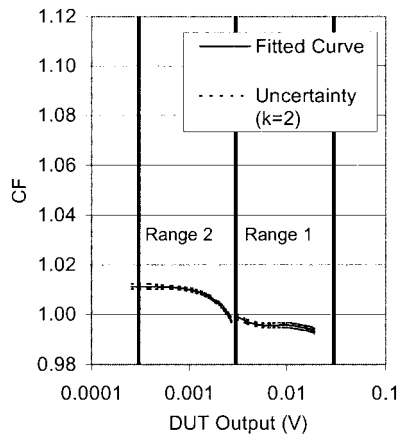


Fig. 9. Detector 2 measured in two meter ranges. The nonlinearity in Range 1 is $\sim 0.6\%$ and 1.4% in Range 2. A range discontinuity of $\sim 0.3\%$ can be seen.

make it easy to compare the magnitude and behavior of the nonlinearities of these detectors. Each detector was measured in more than one span. In Figs. 9–11 the meter measurement ranges are separated by thick black vertical lines where the range discontinuity can be estimated. Because the nonlinearity $CF(V)$ at one particular meter output depends on the calibration or reference point of the measurement, and that point is different for the detectors shown, it is more appropriate to look at the overall (minimum-to-maximum) performance of the nonlinearity of the detectors. The four detectors were measured at different energy levels that do not cover their full measurement ranges, so the results shown here may not represent the general performance of each detector. Detector 1 was measured in one range of the meter with two measurement spans. The nonlinearity in the measured range was $\sim 2.5\%$. The uncertainty with a sharp change at the middle of the curve was due to match-

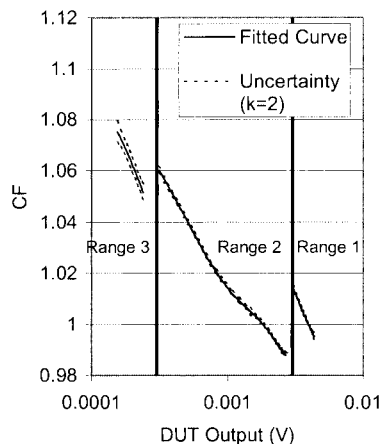


Fig. 10. Measurement of Detector 3 covers one full and two half-meter ranges. This detector exhibits a much larger nonlinearity (8%) and range discontinuity (2%). The nonlinearity behavior is almost the same in the three ranges and has a feature of the effect of background readings.

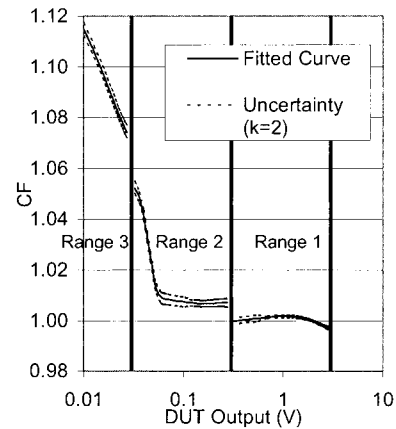


Fig. 11. Measurement of Detector 4 covering approximately 2.5 meter ranges. In Range 1 the detector has a relatively small nonlinearity of $\sim 0.4\%$. In the higher half of Range 2 the nonlinearity is very small, $\sim 0.2\%$, but in the lower half the nonlinearity increases significantly with a decreasing output reading. This is typical of the background effect. This feature of background effect continues in Range 3. The overall nonlinearity is more than 10%. The range discontinuities are also high at approximately 1% and 2%.

ing of the two measurement spans. There were similar changes of uncertainty in Figs. 9–11 although many were not easily discernible due to the small matching uncertainty. Detector 2 in Fig. 9 shows the best nonlinearity performance with $\sim 2\%$ overall nonlinearity over approximately two meter ranges. Its range discontinuity was also very small. Detector 4 in Fig. 11 also showed a small nonlinearity of less than 2% in its highest meter range (300 mV to 3 V). However, it exhibited a dramatic increase in nonlinearity when the output voltage decreased to less than 50 mV. Its nonlinearity reached more than 10% at ~ 10 mV. This nonlinearity behavior is typical of the existence of background response, and this detector does not have the function of background subtraction. Detector 3 also exhibited similar behavior. The large nonlinearity at the lowest end of the meter measurement range of these two detectors indicated that the background effect might be common in pulsed energy meters. Background readings did not register when the magnitude of the noise was not large enough to trigger the meter reading. This effect caused the background to be ignored in the absence of the signal. However, background was present as part of the output when the meter was triggered by large signal pulses. These examples do show that nonlinearity measurement can reveal the existence of the background and correct its effect on the measurement. Detectors 3 and 4 also had a large range discontinuity from 0.5% to 2%. The range discontinuity showed up automatically in the resulting $CF(V)$ during the measurement by switching the meter range at appropriate energy levels. This is one of the advantages of the correlation method over the other methods, where an extra step of measuring range discontinuity is required.⁶

6. Conclusions

We have developed the correlation method and a corresponding system to measure optical detector nonlinearity in the UV range. With this method we have measured directly the correction factor $CF(V)$ on the calibration factor F . The correlation method reduced the effect of the large pulse-to-pulse fluctuations of the excimer UV laser and delivered results with acceptable measurement uncertainties. Measurements where this method was used revealed nonlinearities, range discontinuities, and effects of background reading of some UV detectors. The method and the system extend the calibration of UV detectors to several decades of measurement ranges with reasonable uncertainties.

H. Laabs gratefully acknowledges the support of a Feodor-Lynen fellowship from the Alexander von Humboldt Foundation. H. Laabs had a guest researcher agreement with the National Institute of Standards and Technology from June 2000 until May 2002.

We thank Robert Phelan for insightful discussions of the background effects of pyroelectric detectors.

References

1. R. W. Leonhardt and T. R. Scott, "Deep-UV excimer laser measurement at NIST," in *Integrated Circuit Metrology, Inspection, and Process Control IX*, M. H. Bennett, ed., Proc. SPIE **2439**, 448–459 (1995).
2. R. W. Leonhardt, "Calibration service for laser power and energy at 248 nm," NIST (Nat. Inst. Stand. Technol.) Tech. Note 1394 (U.S. GPO, Washington, D.C., 1998).
3. M. L. Dowell, C. L. Cromer, R. W. Leonhardt, and T. R. Scott, *Characterization and Metrology for ULSI Technology*, D. G. Seiler, A. C. Diebold, W. M. Bullis, T. J. Shaffner, R. C. McDonald, and E. J. Walters, eds. (American Institute of Physics, New York, 1998), pp. 530–541.
4. M. L. Dowell, C. L. Cromer, R. D. Jones, D. A. Keenan, and T. R. Scott, *Characterization and Metrology for ULSI Technology: 2000*, D. G. Seiler, A. C. Diebold, T. J. Shaffner, R. McDonald, W. M. Bullis, P. J. Smith, and E. M. Secula, eds. (American Institute of Physics, New York, 2001), pp. 361–363.
5. H. Laabs, R. Jones, and M. Dowell, "Dose-meter calibration system for 193 nm," at Eighth International Conference on New Developments and Applications in Optical Radiometry, Gaithersburg, Md., 20–24 May 2002.
6. I. Vayshenker, S. Yang, X. Li, and T. R. Scott, "Nonlinearity of optical power meters," NIST (Nat. Inst. Stand. Technol.) Spec. Publ. 905 (U.S. GPO, Washington, D.C., 1996).
7. L. Coslovi and F. Righini, "Fast determination of the nonlinearity of photodetectors," *Appl. Opt.* **19**, 3200–3203 (1980).
8. X. Li, T. R. Scott, S. Yang, C. L. Cromer, and M. L. Dowell, "Nonlinearity measurements of high-power laser detectors at NIST," *J. Res. Natl. Inst. Stand. Technol.* **109**, 429–434 (2004).
9. S. Yang, I. Vayshenker, X. Li, T. R. Scott, and M. Zander, "Optical detector nonlinearity: simulation," NIST (Nat. Inst. Stand. Technol.) Tech. Note 1376 (U.S. GPO, Washington, D.C., 1995).
10. X. Deng, X. Liang, Z. Chen, W. Yu, and R. Ma, "Uniform illumination of large targets using a lens array," *Appl. Opt.* **25**, 377–381 (1986).
11. Y. Ozaki and K. Takamoto, "Cylindrical fly's eye lens for intensity redistribution of an excimer laser beam," *Appl. Opt.* **28**, 106–110 (1989).
12. M. G. Natrella, "Experimental statistics," Natl. Bur. Stand. (U.S.) Handb. 91 (U.S. GPO, Washington, D.C., 1963).
13. B. N. Taylor and C. E. Kuyatt, "Guidelines for evaluating and expressing the uncertainty of NIST measurement results," NIST (Nat. Inst. Stand. Technol.) Tech. Note 1297 (U.S. GPO, Washington, D.C., 1994).